図3-2◆認知症の重症度とBPSD:アルツハイマー型認知症の場合

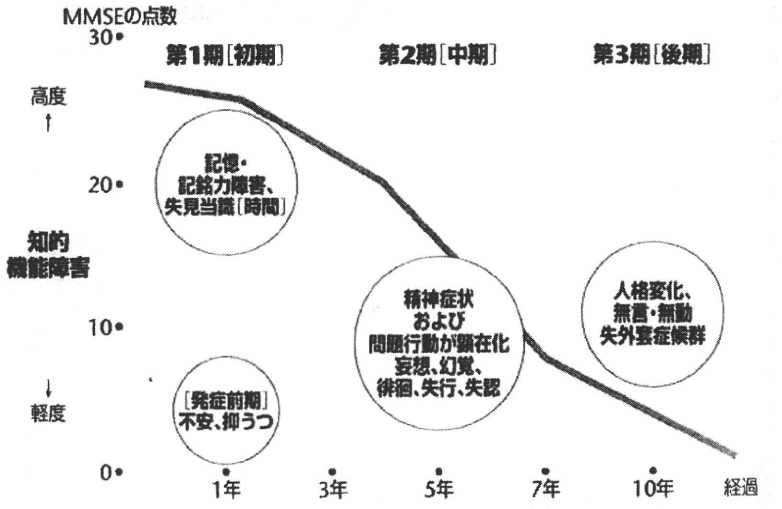

中核症状が著しく進展した後期になると、激しい興奮や多動傾向は少なくなって、意欲低下、無言・無動傾向が強くなり、1日中横になっていたり、食事をとらなくなることが頻繁にみられます。このように病気の経過とともに出現してくるBPSDも大きく変化するのが認知症の特徴です。

認知症の原因は多岐にわたりますが、疾患ごとにBPSDにある程度の差がみられます。血管性認知症ではうつや自発性低下の出現頻度が高いのですが、障害部位によっては焦燥や易怒性が増してくる症例もあります。レビー小体型認知症では幻視が多く、80%の患者に発現するとされています。前頭側頭型認知症では、前頭葉の障害による無気力、自発性低下が中心ですが、同じことを繰り返す常同行為や焦燥・攻撃性も高頻度に認められます。

BPSDの対応について[非薬物的対応、薬物療法]

若年性認知症では本人および家族の葛藤も大きく、心身の健康への影響までが危惧される状態となっています。こうした心情を考慮しない治療や対応は、効果がないばかりか、自尊心の低下や挫折感を増大させる結果となります。BPSDへの対応は、患者および家族の心理的葛藤に配慮し、具体的な問題への対応や病状理解の促進を意図したものでなくてはなりません※2。さらに、認知症の経過は長期にわたるため、長い目で見た取り組みが必要となります。

比較的軽度のBPSDに対処するには、最初に非薬物的対応を考慮します。また非薬物的対応は個々の症例に応じて選択し、患者、介護者の希望、尊厳を尊重することが大切です。対応方法を大きく分けると、環境への介入、問題行動に焦点をあてた対応、心理面に焦点をあてた対応があります※3。

環境への介入

認知症の人にとってストレスの少ない物理的環境をつくっていくことが望まれます。まず睡眠覚醒リズムの維持が大切です。昼夜が逆転することで精神症状が急激に悪化することがしばしばみられます。その予防として、通所介護（デイサービス）などを活用して日中の身体活動を増やすことが大切です。さらに、視覚、聴覚などの感覚低下がBPSD発症に結びつきやすいので、補助具使用や本人に認識しやすい環境整備に配慮します。アルツハイマー型認知症では、ものの形の認知機能が低下しますが、色彩の認知は比較的保たれており、ドアの色

などを区別することで迷いやすい状況を改善する方法もあります。

問題行動への対応

まず、対象となる行動が何であり、どのくらいの頻度で、1日のうちのいつ起こるかなどについて十分に調べておく必要があります。例えば、前頭側頭型認知症でよくみられる常同行為を逆利用したルーチン化療法など新しい方法が開発されつつあります。

また、抑うつ、無気力でひきこもり状態となっている患者に対しては、デイサービスがしばしば有効です。その方法論について、今後さらに研究されることが望まれます。

心理面に焦点をあてた対応

心理面に焦点をあてた対応としては、音楽療法、絵画療法、アロマセラピーなどが、抑うつや気分不安定に対して一定の効果が期待できるとされています。

BPSDの治療法として薬物療法は重要な手段です。BPSDは多彩な像を示し、それぞれの状態に応じた薬物の選択が求められます[表3-2]。せん妄、幻覚、妄想、不安、焦燥、徘徊、多動といった激しい行動、多動傾向を示す例には、定型、非定型の抗精神病薬および気分安定化作用を期待しての抗てんかん薬を処方します。有害事象として歩行障害、手のふるえなどの錐体外路症状、ふらつき・眠気、排尿障害に注意します。

アパシーと抑うつとの鑑別が重要であることは前述しましたが、アパシーでは原因となるような身体疾患を除外したうえで、アルツハイ

表3-2◆認知症の薬物療法

BPSD	夜間せん妄	幻覚・妄想	不安・焦燥	徘徊・多動	意欲低下	自発性低下	抑うつ
アセチルコリンエステラーゼ阻害剤［ドネペジル］					○	○	
ブチロフェノン系［ハロペリドール］	○	○	○	○			
SDA［リスペリドン、クエアチピン］*1	○	○	○	○			
ベンズアミド系［スルピリド］		○			○	○	○
SSRI［パロキセチン、フルボキサミン］*2					○	○	○
SNRI［ミルナシプラン］*3					○	○	○
漢方薬［抑肝散］		○	○	○			

［*1］SDA：非定型抗精神病薬［セロトニン、ドパミン拮抗薬］
［*2］SSRI：選択的セロトニン再取り込み阻害薬
［*3］SNRI：セロトニン・ノルアドレナリン再取り込み阻害薬

マー型認知症であれば塩酸ドネペジル（アリセプト）の効果が期待できます。ただし、塩酸ドネペジル（アリセプト）では、徘徊、焦燥、攻撃性を誘発してしまうことあるので、注意が必要です。

抑うつに対しては選択的セロトニン再取り込み阻害薬（SSRI）、セロトニン・ノルアドレナリン再取り込み阻害薬（SNRI）が有効ですが、従来から用いられてきたスルピリドも効果を期待できます。投与時間についても気を遣います。鎮静作用のある薬物は夕方から夜にかけて投与し、脳賦活作用のある薬や利尿剤は朝、昼に最大の効果が出るようにするのがいいでしょう。

若年発症の場合の特徴はあるのか

若年期と老年期のBPSDの頻度はほぼ同じですが、内容は異なっています。若年期に多いBPSDは、徘徊、興奮や大声、意欲低下などで、老年期に多いものは、せん妄、幻覚、妄想などです。若年性認知症の人に対する接し方は、原則的には、老年期の認知症の人と変わりません。患者本人の基本的人権や尊厳を否定しないことや、本人の希望を叶え、自身のもつ能力を十分に発揮できるような環境空間を用意するような方向で働きかけます。

具体的なケア内容としては、社会参加の機会、身体的運動を多く取り入れることのほかに、単なるレクリエーションではなく、仕事やボランティアなど社会活動を取り入れることが重要です[*4]。若年性認知症では身体能力が保たれているため、精神症状、行動障害が制御困難になることが多くなりますが、エネルギッシュな行動はケアプログラムに運動のメニューを加えることで解決に導くようにします。

今後の課題

若年性認知症に伴うBPSDに対して薬物、非薬物の両面からさまざまな試みが行われ、よい結果を生み出している例もあります。しかし、若年性認知症の場合は罹病期間が長期にわたることが予想され、また認知症の一般的特徴として、時間とともに症状が変化し、その対応が求められます。

このような若年性認知症の特性に対応できる専門施設の絶対数が不

足しています。また患者家族が利用できる情報が十分でない点も課題でしょう。認知症そのものの治療・対応だけでなく、経済的・社会的背景にまで踏み込んだ総合的な若年性認知症ケアのための医療・介護連携の構築が求められます。

参考文献

*1
国際老年精神医学会,日本老年精神医学会監訳「モジュール2 臨床的な問題 In 痴呆の行動と心理症状」
pp27-49、アルタ出版、2005年

*2
松田修「若年性アルツハイマー病に対する心理教育的配慮に基づく認知リハビリテーションの事例」
「心理臨床学研究」24、pp559-570、金剛出版、2006年

*3
国際老年精神医学会,日本老年精神医学会監訳
「モジュール5 薬物によらない対応 In 痴呆の行動と心理症状」
pp97-123、アルタ出版、2005年

*4
宮永和夫「若年認知症の治療とケア」「老年精神医学雑誌」
20、pp855-864、ワールドプランニング、2009年

The Effects of a PPARα Agonist on Myocardial Damage in Obese Diabetic Mice With Heart Failure

Rui CHEN,[1,5*] MD, Fengxia LIANG,[2,7*] MD, Shigeto MORIMOTO,[3] MD, Qian LI,[6] MD, Junji MORIYA,[1] MD, Jun-ichi YAMAKAWA,[1] MD, Takashi TAKAHASHI,[1] MD, Kunimitsu IWAI,[3] MD, *and* Tsugiyasu KANDA,[4] MD

SUMMARY

Recent studies have confirmed that PPARα agonists have not brought the anticipated benefits to patients with type 2 diabetes and potentially fatal heart disease. We hypothesized that such agonists may have a cardio-suppressive effect in treating such disorders, therefore, we inoculated diabetic KKAy mice with encephalomyocarditis virus (EMCv) to induce a diabetic model with severe myocardial damage. WY14643, a potent PPARα agonist, was administered intraperitoneally either simultaneously (WY14643-late group) or 3 days before viral inoculation (WY14643-early group). WY14643-treated mice, especially those in the WY14643-early group, had higher mortality than those in the vehicle-treated group (vehicle) in the first 5 days after EMCv inoculation. However, the survival rate in the vehicle group decreased rapidly after day 4 and was the lowest of all 3 groups by day 9. The WY14643-treated mice showed reduced body weight and blood glucose, improved myocardial pathological changes, lower cardiac TNF-α expression, and significantly higher adiponectin expression, whereas the LW/LC ratio was lower and cardiac UCP3 mRNA expression higher in the WY14643 treatment groups than in the vehicle group on day 4. WY14643 therefore has cardioprotective and cardio-suppressive effects when used to treat EMCv-induced myocarditis in diabetic mice. The cardioprotective effect may be due to its anti-inflammatory properties and its ability to increase cardiac adiponectin expression, whereas the reduced cardiac efficiency may be due to its enhancement of cardiac UCP3 mRNA expression. (Int Heart J 2010; 51: 199-206)

Key words: Tumor necrosis factor-α (TNF-α), Adiponectin, Uncoupling protein 3 (UCP3)

Peroxisome proliferator-activated receptorα (PPARα) belongs to the nuclear receptor superfamily and is known to regulate the expression of genes for the transport proteins and enzymes that participate in inflammation and metabolism.[1] It has been shown that PPARα agonists are capable of decreasing the production of some inflammatory cytokines, such as tumor necrosis factor-α (TNF-α) in cardiac myocytes.[2] Moreover, the potent PPARα agonist WY14643 can directly increase the expression of adiponectin receptors in white adipose tissue, which bind with adiponectin and exert antidiabetic, antiatherosclerotic, and anti-inflammatory effects.[3] Likewise, recent reports have indicated that PPARα agonists can improve the survival rate of experimental animals with heart failure.[4]

The Fenofibrate Intervention and Event Lowering in Diabetes (FIELD) study, however, found that PPARα agonists had not brought the anticipated benefits to heart failure in type 2 diabetic patients and had even increased the death rate due to fatal cardiac disease, although to a statistically insignificant degree,[5] thus suggesting that PPARα agonists may have some adverse effects on myocardial damage or cardiac function despite their cardioprotective effects.

Uncoupling proteins (UCPs) are inner mitochondrial membrane proteins that play a role in dissipating the mitochondrial proton gradient by allowing protons to re-enter the mitochondrial matrix without the concomitant synthesis of ATP. Three such proteins—UCP1, UCP2, and UCP3—are known.[6] We are interested in UCP3 because it is mainly expressed in heart and skeletal muscle and is involved in the regulation of biological processes associated with mitochondrial energy metabolism.[7] Indeed, increased UCP3 levels have been reported to correlate with higher myocardial consumption and reduced cardiac efficiency.[8] WY14643 can increase the level of UCP3 mRNA in liver and brown fat tissue of KKAy mice.[3] Likewise, myocardial levels of UCP3 in BALB/c mice increased by 54% upon treatment with WY14643.[9] WY14643 may therefore exacerbate heart failure by increasing UCP3 expression, although more evi-

From the [1] Departments of General Medicine, [2] Endocrinology, [3] Geriatric Medicine and [4] Community Medicine, Himi City Hospital, Kanazawa Medical University, Toyama, Japan [5] Department of Traditional Chinese Medicine, Union Hospital, [6] School of Public Health, Tongji Medical College, Huazhong University of Science and Technology, and [7] Hubei College of Traditional Chinese Medicine, Wuhan, China. * These authors contributed equally to this work.

This study was supported in part by a grant for Promoted Research from Kanazawa Medical University (S2005-5), a Grant-in-Aid for Scientific Research (C) from the Ministry of Education, Science, Sports, and Culture of Japan (no. 17590767), and a grant from the Chinese Postdoctoral Science Foundation (no. 20070420179). This work was supported by a Grant-in-Aid for Scientific Research from the Ministry of Education, Science, Sports and Culture of Japan to T.K. (no. 19590835) and by a Grant for Project Research of Kanazawa Medical University (H2010-13).

Address for correspondence: Tsugiyasu Kanda, MD, Department of Community Medicine, Himi City Hospital, Kanazawa Medical University, 31-9 Saiwai-cho, Himi, Toyama 935-8531, Japan.

Received for publication September 10, 2009.
Revised and accepted February 19, 2010.

dence is needed in the event of diabetes complicated with fatal heart disease.

Some metabolic diseases, such as type 2 diabetes and obesity, predispose to heart failure, and inflammation plays an important role in the association between them.[10] Encephalomyocarditis virus (EMCv) can induce severe myocarditis and heart failure in experimental animals.[11] In previous studies, we inoculated EMCv into obese mice to set up a model of obese mice with severe heart failure, and found higher TNF-α and lower adiponectin expression levels in the injured myocardium.[12,13] Herein, obese diabetic KKAy mice inoculated with EMCv were used to induce a model of type 2 diabetes and obesity complicated with severe heart failure, and subsequently to evaluate the effect of WY14643. We determined the survival rate and examined the expression levels of cardiac TNF-α, adiponectin, and UCP3 at different stages of myocardial damage and found that WY14643 plays different roles in the injured heart.

Methods

Animals and treatments: Eight-week-old female KKAy mice weighing 38-42 g were purchased from Clea Japan Inc. (Tokyo), and maintained with food and water *ad libitum*. These mice were randomly divided into 3 groups: a WY14643-early group, which received WY14643 (Sigma, USA) at a daily dose of 50 mg/kg starting 3 days before viral inoculation, and a WY14643-late group and vehicle treatment group (vehicle), which received WY14643 and vehicle (dimethyl sulfoxide), respectively, simultaneously with viral inoculation. WY14643 (0.1 mL) was administered intraperitoneally once daily. Experimental protocols were approved by the Animal Experimental Committee of Kanazawa Medical University.

Study design: The study consisted of two experiments. Experiment 1 was performed to determine the survival rate and any change in body weight (BW). In this experiment, 21, 28, and 19 mice were raised in the vehicle, WY14643-early, and WY14643-late groups, respectively. The survival rate and BW were recorded daily from 3 days before EMCv inoculation. The endpoint was a survival rate of less than 20% in any group. Experiment 2 was designed to obtain plasma and tissue samples on days 0, 4, and 9 after EMCv inoculation, with 45 mice in the vehicle group, 39 in the WY14643-early group, and 18 in the WY14643-late group. Eight KKAy mice without inoculation and treatment were used as normal control (control) and sacrificed on day 0.

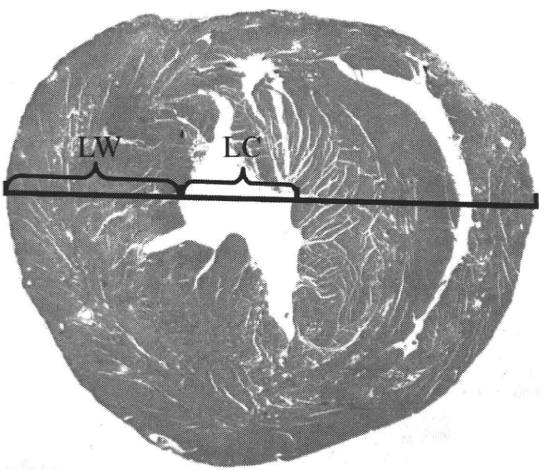

Figure 1. Measurement of left ventricular wall thickness and cavity dimension. LW indicates left ventricular wall and LC, left cavity.

EMCv and inoculation protocol: A myocarditic variant of EMCv was provided by Dr. Y. Seto, Institute for Advanced Medical Research of Keio University (Tokyo). Virus preparations and inoculation were performed as described previously.[13]

Histological heart examinations: The BW and heart weight (HW) of each mouse was recorded at sacrifice in experiment 2. The heart was transversely divided into two halves. One half, which included the cardiac apex, was stored at -80°C until use, while the other half was fixed in 10% buffered formalin and blocked with paraffin for histological examination and immunohistochemical study. After fixation, the heart was transversely sectioned at the maximal circumference of the ventricle. Some slices were stained with hematoxylin-eosin to assess the severity of myocardial necrosis and inflammatory cell infiltration according to previously described scales.[13,14]

The LV wall thickness (LW) and LV cavity (LC) dimensions were measured with the slice at the maximal circumference of the ventricle, as described by Matsumori, *et al*[15] (Figure 1). The diameter of the myocardial fiber in the lateral LV wall was determined as described previously.[13]

Blood glucose (BG) and plasma free fatty acid (FFA): BG and plasma FFA were determined with a Fuji Dry Chem System (Medical System Co., Tokyo) and nonesterified fatty acid-C test kit (Wako Pure Chemical Industries, Osaka, Japan), respectively.

Immunohistochemical examination: To identify the anatomic localization and expression levels of TNF-α, adiponectin, and UCP3 within the myocardium, immunohistochemistry was performed using the avidin biotin complex methods (Vectastain ABC kit, Vector Laboratories, Burlingame, CA), as described previously.[14] All sections were previously blocked with normal goat serum for 20 minutes at room temperature to minimize background staining. The slides were then incubated with anti-human TNF-α mouse monoclonal antibody clone 4H31 (#HM2010, HyCult Biotechnology b.v., Uden, the Netherlands), anti-human adiponectin mouse monoclonal antibody clone (#ab22554, Abcam, Tokyo), and UCP3 rabbit polyclonal antibody #ab10985, Abcam, Japan). Sections were counterstained with hematoxylin. The slides were reviewed blind by the same pathologist and graded semiquantitatively according to the degree of immunoreactivity: 0 for absence of staining, 1 for weak, 2 for moderate, and 3 for strong staining.[16] They were then compared with the respective control slides to exclude nonspecific staining.

Comparative expression of TNF-α, adiponectin, and UCP3 mRNA in heart tissue: RNA extraction from the frozen cardiac tissue was performed following the manufacturer's protocol (RNeasy Mini Kit, QIAGEN Inc., Tokyo). DNAase was applied during RNA extraction to avoid DNA

contamination. Total RNA concentration was determined by measuring the optical density at 260 and 280 nm. Aliquots of 20 μL RNA from each tissue sample were used to produce cDNA. Comparative expression levels of TNF-α, adiponectin, and UCP3 mRNA in cardiac tissue from each group were determined using quantitative real-time reverse transcriptase-polymerase chain reaction (RT-PCR). A TaqMan minor groove binding (MGB) Probe (Applied Biosystems Inc., CA, USA) was applied for real-time PCR, and a commercially available kit was used for TNFα, adiponectin, and UCP3 RT-PCR (Applied Biosystems Inc.). Primers and TaqMan probes for the target gene (TNFα, adiponectin, and UCP3) and internal reference gene (Rodent GAPDH) were purchased from Applied Biosystems (TaqMan® Gene Expression Assays). Each TaqMan probe was labeled with a reporter dye [6-carboxyfluorescein (FAM)] situated at the 5' end of the oligonucleotide and a quencher dye (MGB) located at the 3' end. TaqMan® Gene Expression Assay numbers for TNF, adiponectin, and UCP3 were Mm00443258mL, Mm00456425mL, and Mm00494074mL, respectively (Applied Biosystems Inc.). Quantification of target cDNA (TNFα, adiponectin, and UCP3) and GAPDH was performed in 96-well plates using an ABI PRISM7500 Sequence Detection System (ABI); data collection and analysis was performed using the machine's software. PCR was carried out on a final volume of 25 μL containing cDNA equivalent to 10-100 ng of total RNA, 10 μL of 2 × TaqMan Fast PCR Master Mix, and 1 μL of 20 × TaqMan Expression Assay reagent. Each sample was analyzed in triplicate. The thermal cycler conditions were 95°C for 20 seconds, followed by 40 cycles at 95°C for 3 seconds, and 60°C for 30 seconds. The comparative C_T method of data analysis was used to analyze the data. C_T is the PCR cycle at which an increase in reporter fluorescence above the baseline level was first detected. C_T values for the target and internal reference gene were calculated for each sample along with the difference between these values (ΔC_T). $\Delta\Delta C_T$ was calculated as the difference in ΔC_T between sample and calibrator sample. The amount of target gene expression, normalized to an internal reference and relative to calibrator, was given by: $2^{-\Delta\Delta CT}$.

Statistical analysis: The Kaplan-Meier analysis and a log rank test were used to assess the survival rate of mice in each group. Other data are expressed as the mean ± SEM and were analyzed by ANOVA. When results were found to be significant, comparisons were performed using the Bonferroni test. Statistical significance was defined as $P < 0.05$.

Results

Survival rate and BW in experiment 1: According to the Kaplan-Meier analysis, WY14643-treated mice, especially those in the WY14643-early group, had higher mortality than those in the vehicle group in the first 5 days after EMCv inoculation, although the survival rate in the vehicle group decreased rapidly after day 4 and was the first to drop

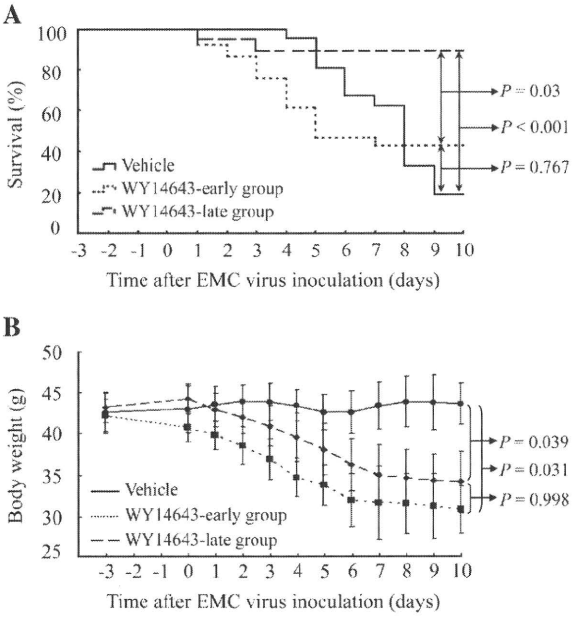

Figure 2. A: Results of the Kaplan-Meier survival analysis showing the lower mortality during the later stages, and the higher mortality during the earlier stages, of myocarditis in the WY14643 treatment groups than in the vehicle group. **B:** Treatment with WY14643 decreased the body weight of KKAy mice significantly.

Table I. Effects of WY14643 on Body Weight (BW), Heart Weight (HW), Blood Glucose (BG), and Plasma Free Fatty Acid (FFA) in KKAy Mice With Acute Viral Myocarditis

	n	BW (g)	HW (mg)	HW/BW (%)	BG (mmol/L)	FFA (mEq/L)
Day 0						
Control	8	38.4 ± 2.0	152.7 ± 16.8	0.40 ± 0.02	7.07 ± 0.18	1.05 ± 0.12
WY14643-early	8	35.4 ± 2.1$^{\#}$	132.0 ± 7.5$^{\#}$	0.37 ± 0.03	3.63 ± 1.05$^{\#\#}$	1.19 ± 0.03$^{\#}$
Day 4						
Vehicle	8	38.0 ± 4.4	174.3 ± 7.1	0.46 ± 0.05	14.13 ± 4.74	1.43 ± 0.05
WY14643-early	8	33.1 ± 2.0*	119.5 ± 10.1**	0.36 ± 0.03*	1.81 ± 0.49**	1.21 ± 0.09*
WY14643-late	8	34.8 ± 0.6*	143.3 ± 27.5*	0.41 ± 0.08	2.28 ± 1.04**	1.80 ± 0.06*†
Day 9						
Vehicle	7	43.6 ± 2.2	153.4 ± 13.0	0.35 ± 0.02	10.66 ± 2.09	1.84 ± 0.10
WY14643-early	9	33.0 ± 3.3**	114.3 ± 9.1**	0.35 ± 0.01	6.09 ± 1.17**	1.47 ± 0.13**
WY14643-late	8	36.0 ± 3.6*	141.5 ± 11.1*	0.40 ± 0.05	7.32 ± 2.79*	1.48 ± 0.16**

$^{\#}P < 0.05$, $^{\#\#}P < 0.01$ with respect to control; $^{*}P < 0.05$, $^{**}P < 0.01$ with respect to vehicle on the corresponding day; $^{\dagger}P < 0.01$ with respect to WY14643-early group.

below 20% (day 9; Figure 2A). Days 4 and 9 were therefore chosen as the sacrifice days in experiment 2.

WY14643-early and -late treatment had similar effects on the BW of KKAy mice, with the BW decreasing significantly after the injection of WY14643 to reach statistical significance on day 9 (Figure 2B).

BW and HW in experiment 2: After 3 days of prior treatment, the HW/BW ratio was lower in the WY14643-early group than in the control group, although the difference was not statistically significant. The HW in the two WY14643 treatment groups was markedly lower than in the vehicle group on day 4, although statistical significance was only found between the WY14643-early and vehicle groups after normalization by BW. The HW on day 9 was significantly lower in the two treatment groups than in the vehicle group, whereas HW/BW showed no significant differences between the 3 groups (Table I).

Pathological findings: Myocardial lesions and inflammatory cell infiltration were present in EMCv-inoculated KKAy mice sacrificed on days 4 and 9 (Figure 3). The pathological scores (Figure 4A) and number of infiltrating cells (Figure 4B) showed that treatment with WY14643 reduced the severity of the inflammation on both days, and was statistically significant on day 9.

As shown in Table II, LW, LC, and their ratio (LW/LC) were lower in the WY14643-early group than in control, with the latter two reaching statistical significance. The LW was smaller and the LC larger in the WY14643 treatment groups on day 4 than those in vehicle, with the comparison between the WY14643-late group and vehicle groups reaching statistical significance. The LW/LC ratio was therefore lower in the WY14643 treatment groups than in vehicle on day 4. The LC in the vehicle group on day 9 was markedly higher than for either the WY14643-early group or -late group, which means that the LW/LC ratio in the vehicle group was significantly smaller than for either of the other two groups. No significant difference was found between the WY14643-early and -late groups as regards LW, LC, and LW/LC on either day 4 or day 9.

The LV myocardial fiber diameters were smaller in the WY14643-early group than in the control on day 0, although the difference was not statistically significant. The diameters in the WY14643-late group on days 4 and 9 were significantly lower than those in vehicle ($P < 0.01$), and this significance also existed between the vehicle and WY14643-early groups on day 4, although not on day 9. The myocardial diameters in the WY14643-late group were significantly lower than those in the WY14643-early group

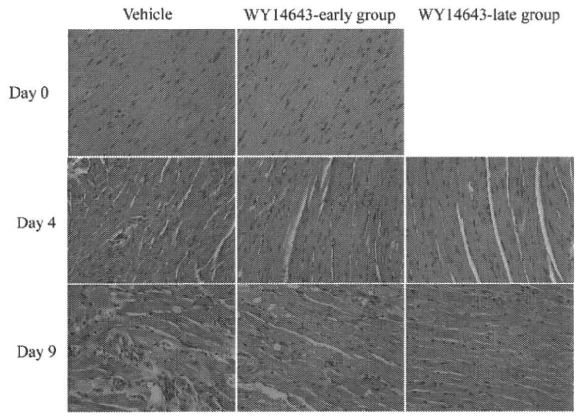

Figure 3. Cardiac pathological findings for KKAy mice on days 0, 4, and 9. Myocardial necrosis with inflammatory cell infiltration was found after viral inoculation. Treatment with WY14643 reduced the inflammation in heart tissue.

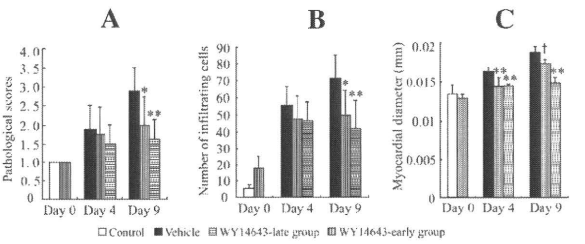

Figure 4. A: The pathological scores for heart tissue; **B:** the number of infiltration cells at high magnification (400 ×); **C:** the diameter of myocardial fibers in KKAy mice. Myocardial necrosis, pathological score, and the number of infiltration cells on day 9 were lower in the two WY14643 treatment groups, especially in the late treatment group. LV myocardial fiber diameters were greater in the vehicle group than in the two WY14643 treatment groups. $^{*}P < 0.05$, $^{**}P < 0.01$, $^{\dagger}P > 0.05$ with respect to vehicle.

Table II. Left Ventricular Wall Thickness (LW) and Cavity Dimension (LC), and Their Ratios

	n	LW (mm)	LC (mm)	LW/LC
Day 0				
Control	8	2.19 ± 0.45	1.21 ± 0.53	1.83 ± 0.36
WY14643-early group	8	2.01 ± 0.65	1.51 ± 0.07$^{\#}$	1.33 ± 0.49$^{\#}$
Day 4				
Vehicle	8	2.23 ± 0.28	0.57 ± 0.21	3.84 ± 2.12
WY14643-early group	8	1.97 ± 0.46	0.84 ± 0.31	2.33 ± 0.66
WY14643-late group	8	1.96 ± 0.44*	0.93 ± 0.12*	2.11 ± 0.27*
Day 9				
Vehicle	7	2.07 ± 0.22	1.51 ± 0.29	1.37 ± 0.25
WY14643-early group	9	1.95 ± 0.35	1.35 ± 0.46*	1.45 ± 0.63*
WY14643-late group	8	1.89 ± 0.53*	1.26 ± 0.44**	1.50 ± 0.55**

$^{\#}P < 0.05$ with respect to control; $^{*}P < 0.05$, $^{**}P < 0.01$ with respect to vehicle on the corresponding day.

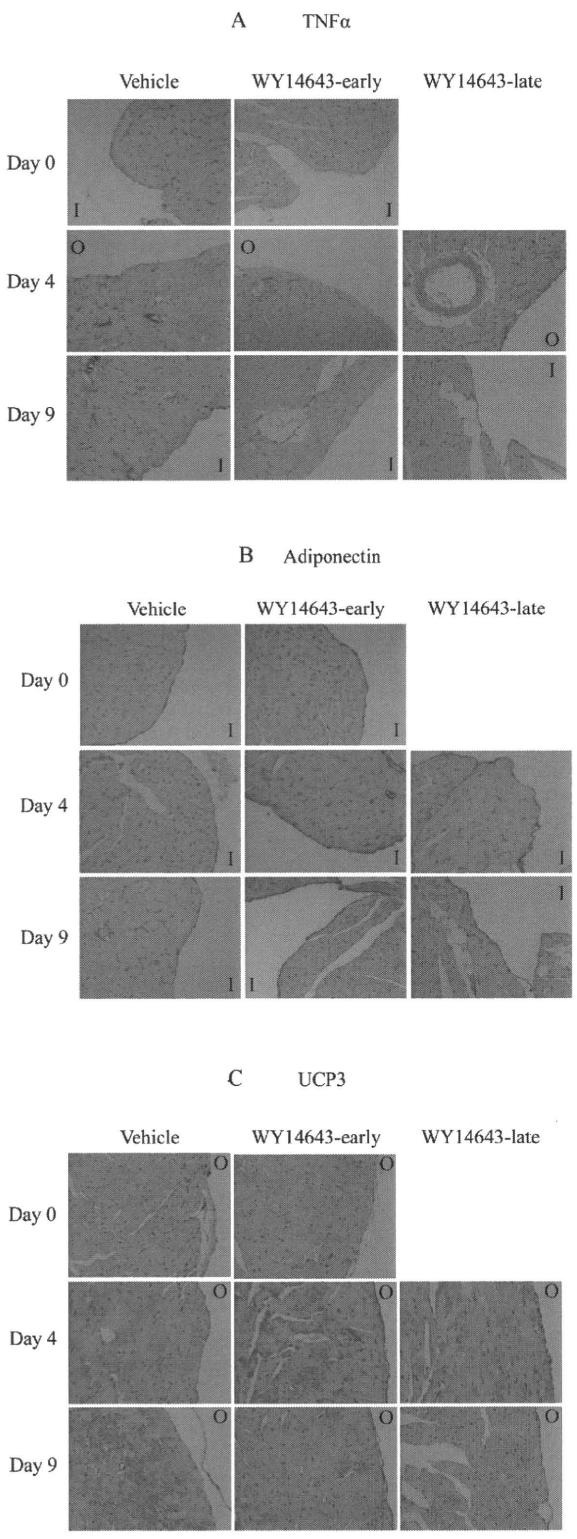

Figure 5. Immunohistochemical findings. Cardiac expression of TNF-α, adiponectin, and UCP3 is shown in A, B, and C respectively (magnification: 400 ×). I represents inner heart and O represents outer heart.

on day 9 (Figure 4C).

BG and plasma FFA: As shown in Table I, WY14643 treatment significantly ameliorated hyperglycemia in KKAy mice, with no significant difference being found between the two treatment groups. Interestingly, WY14643 increased plasma FFA levels on day 0 in the WY14643-early group and on day 4 in the WY14643-late group, but significantly decreased FFA levels on day 4 and day 9 in the WY14643-early group and on day 9 in the WY14643-late group.

Immunohistochemical findings: Cardiac TNF-α was positive in the vehicle group on days 4 and 9 but only weakly positive in the WY14643-early and WY14643-late group (Figure 5A); cardiac expression of adiponectin protein was more strongly positive in the two WY14643 treatment groups than that in the vehicle group (Figure 5B). Cardiac UCP3 was more strongly positive on day 4 in the two WY14643 treatment groups, but more strongly positive on day 9 in the vehicle group (Figure 5C). Cardiac adiponectin and UCP3 were positive on day 0, whereas TNF-α was nearly negative in the vehicle and WY14643 treatment groups (Figures 5A, 5B and 5C).

TNF-α, adiponectin, and UCP3 mRNA expression in heart tissue: The comparative expression levels of TNF-α, adiponectin, and UCP3 mRNA in heart tissue on days 0, 4, and 9 after EMCv inoculation are shown in Figure 6. Significantly higher levels of TNF-α mRNA were observed on days 4 and 9 in EMVc-inoculated mice, with WY14643 treatment reducing this increase markedly, especially on day 9. The expression levels of adiponectin mRNA were significantly enhanced by WY14643 treatment on days 0, 4, and 9. Three days of prior WY14643 treatment increased the UCP3 mRNA expression levels significantly with re-

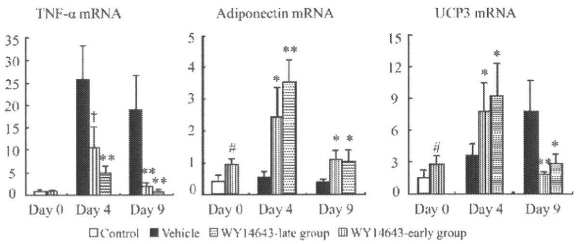

Figure 6. Expression of cardiac TNF-α , adiponectin, and UCP3 mRNA by R-PCR. $^{*}P < 0.05$, $^{**}P < 0.01$, $^{\dagger}P = 0.059$ with respect to vehicle; $^{\#}P < 0.05$ with respect to control.

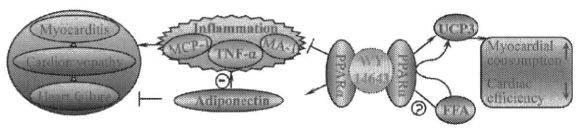

Figure 7. The dual effect of WY14643 on acute viral myocarditis and heart failure in obese diabetic mice. The cardioprotective effect of WY14643 may contribute to reduced inflammatory[3] and increased cardiac adiponectin levels, whereas the reduced cardiac efficiency may be due to up-regulation of UCP3 mRNA expression. ← denotes promotion and ⊣ inhibition. MCP-1 indicates monocyte chemoattractant protein-1; MA-1, macrophage antigen-1; FFA, free fatty acid; and UCP3, uncoupling protein 3.

spect to those in control on day 0. UCP3 mRNA expression levels were significantly higher on day 4, but lower on day 9, in the two treatment groups than those in the vehicle group. No significant difference was found between the two WY14643 treatment groups as regards cardiac TNF-α, adiponectin, and UCP3 mRNA expression on days 4 and 9.

Discussion

The above results demonstrate that the PPARα agonist WY14643 has different effects on the survival of obese diabetic mice with EMCv-induced heart failure. Thus, simultaneous WY14643 treatment increased the survival rate at the endpoint of experiment 1 mainly due to its anti-inflammatory effects and its enhancement of cardiac adiponectin expression, whereas WY14643-treated mice, especially those in the WY14643-early group, had high mortality in the first 5 days after viral inoculation, possibly as a result of the higher UCP3 levels leading to reduced cardiac efficiency (Figure 7).

The survival rate in our study was similar to that in previous clinical and experimental reports. For example, although fenofibrate, another well-known PPARα agonist, reduced the risk of nonfatal myocardial infarctions and coronary revascularisations in patients with type 2 diabetes in the FIELD study, sudden cardiac deaths and deaths from heart failure numbered 54 and 11, respectively, in the placebo group and 70 and 13, respectively, in the fenofibrate group.[5] In an animal experiment, Ichihara, *et al* reported that the survival rate for heart-damaged mice was slightly lower in one of the fenofibrate treatment groups than in the vehicle group at 13 weeks, although the survival rates were significantly higher in the treatment groups than in the vehicle group at 18 weeks.[4] All these results suggest that PPAR ± agonists have a dual effect on the impaired heart.

Inflammation is one of the pivotal factors contributing to the transition from myocarditis and cardiomyopathy to heart failure, therefore, anti-inflammatory treatments play an important role in preventing this transition.[17] Recent studies have revealed that WY14643 is capable of inhibiting inflammation in white adipose tissue by suppressing the expression of TNF-α, monocyte chemoattractant protein-1, and macrophage antigen-1.[3] These inflammatory cytokines are also implicated in myocarditis, dilated cardiomyopathy, and heart failure.[18,19] In our recent study, EMCv inoculation into KKAy mice induced severe inflammation in heart tissue and heart failure, which was strongly associated with increased local TNF-α levels.[12] In this study, high pathological scores, a large number of infiltrating cells, and a higher LC/LW ratio were found in viral-inoculated KKAy mice on day 9. Treatment with WY14643 ameliorated the inflammation in cardiac tissue and reduced the LC/LW ratio by inhibiting TNF-α expression, which might result in a beneficial effect as regards myocarditis, dilated cardiomyopathy, and heart failure, and thereby decrease the mortality.

Adiponectin has recently also been found to be expressed by cardiomyocytes, and the locally produced hormone could be involved in the regulation of cardiac metabolism and function[20] and myocardial hypertrophy.[21] Our previous study showed that adiponectin was expressed in injured myocytes in autopsy cases[22] and that suppressed cardiac adiponectin mRNA expression in obese mice was associated with the development of acute EMCv-induced myocarditis.[12] An elevated local expression of adiponectin in cardiac tissue can decrease the severity of myocardial injury associated with the attenuation of cardiac hypertrophy and inflammation in obese mice with acute viral myocarditis.[13] In agreement with this previous study, we found that adiponectin mRNA expression levels were markedly higher in WY14643-treated mice on days 0, 4, and 9, and that the myocardial diameter decreased and the inflammation improved. These findings imply that the adiponectin-associated antihypertrophic and anti-inflammatory effects might be involved in WY14643 treatment of EMCv-inoculated KKAy mice.

UCP3 is a recently identified member of the mitochondrial transporter superfamily that is expressed predominantly in heart and skeletal muscle to inhibit the synthesis of ATP in these tissues.[23] An elevated expression of local UCP3 has been reported to correlate with increased myocardial oxygen consumption and reduced cardiac efficiency.[8] Murray, *et al* reported that high plasma FFA can increase cardiac UCP3 levels via a PPARα-dependent mechanism.[9] Previous reports concerning the effect of WY14643 on plasma FFA levels are contradictory.[3,9] For example, Tsuchida, *et al* reported that an 8-week treatment with WY14643 decreased serum FFA levels significantly in KKAy mice,[3] whereas Murray, *et al* found that a one-week treatment with WY14643 did not reduce plasma FFA levels, although they found a nonsignificant increase in wild-type mice,[9] We found that the plasma FFA levels in KKAy mice increased significantly in the WY14643-early group on day 0 (after 3 days of treatment) and in the WY14643-late group on day 4, but decreased significantly in the WY14643-early group after 7 and 12 days of treatment (on days 4 and 9) and in the WY14643-late group after 9 days of treatment (on day 9). The cardiac UCP3 levels therefore appear to vary with plasma FFA levels in a PPARα-dependent manner, as reported by Murray, *et al*,[9] who also found that WY14643 treatment increased myocardial UCP3 levels in wild-type mice by 54%. In our study, WY14643 treatment increased the expression of UCP3 mRNA in cardiac tissue on days 0 and 4, but decreased it on day 9, which might be due to the combined effect of WY14643 and plasma FFA on PPARα. The increased UCP3 level on day 4 might further decrease ATP synthesis in the inflamed myocardium in WY14643-treated mice, and may therefore be responsible for the lower contractile movement and ATP-dependent iron transport. This would aggravate the heart failure and might be a predictor for the higher mortalities on day 4 in the two WY14643 treatment groups than in vehicle.[24]

As indicated in Table I and Figure 6, 3 days of prior treatment in the WY14643-early group increased plasma FFA levels and cardiac UCP3 mRNA expression, which enhanced myocardial consumption and reduced cardiac ATP production. In the WY14643-late group, however, the plasma FFA levels, cardiac UCP3 mRNA expression, and heart efficiency were the same as those in the control group when attacked by EMCv on day 0, which means that although the heart was protected by the anti-inflammatory effects and increased adiponectin levels equally in the two treatment

groups during the initial few days of treatment, the heart efficiency was lower in WY14643-early mice. Moreover, WY14643 treatment could significantly replace cardiac n-3 polyunsaturated fatty acids (PUFA) by n-6 PUFA, which would be detrimental to the heart since n-3 PUFAs possess cardioprotective and antiarrhythmic properties.[25] In addition, WY14643 treatment might lead to cardiac dysfunction in the diabetic heart by influencing the activity of PPARα.[26] These lines of evidence might be the possible foundation for the higher death rate in the WY14643-early group than in the WY14643-late group.

WY14643 treatment also significantly improved the hyperglycemia and reduced the body weight of KKAy mice. It is well known that cardiovascular disease is the leading cause of death for patients with type 2 diabetes and that maintaining glucose homeostasis is crucial for reducing its mortality.[27] In addition, an increased body-mass index is also associated with an increased risk of heart failure and death.[28] WY14643 therefore appears to improve the survival and heart failure risk for KKAy mice at this point of antihyperglycemia and body weight loss.

The PPARγ signal in mice increased weakly after WY14643 treatment.[29] Likewise, PPARγ ligands have been reported to attenuate AngII-induced cardiac fibrosis.[30] The pathological findings of this study also showed that treated mice had a lower level of fibrosis. Further studies should therefore aim to determine whether this decrease is due to the slight activation of PPARγ or the activation of PPARα.

PPARα agonists such as WY14643 and fenofibrate have very complex biological effects resulting from the activation or suppression of dozens of genes,[1] the biological effects of which remain largely unknown. Despite the fact that this study only provides limited targets for WY14643, its findings suggest that WY14643 has both beneficial and harmful effects on obese diabetic mice with severe myocarditis and heart failure. In addition, both WY14643 and plasma FFA can increase cardiac UCP3 levels by a PPARα-dependent pathway, and WY14643 can also affect the plasma FFA level. Further studies are therefore required to elucidate the competitive binding of WY14643 and plasma FFA to PPARα when WY14643 is used as a therapeutic agent.

Conclusion: This study has shown for the first time the cardioprotective and cardio-suppressive effects of WY14643, a potent PPAR ± agonist, on acute viral myocarditis and heart failure in obese diabetic mice in the initial stages after viral inoculation. The cardioprotective effect of WY14643 may contribute to reduced inflammatory and increased cardiac adiponectin levels, whereas the reduced cardiac efficiency may be due to up-regulation of UCP3 mRNA expression.

Acknowledgments

We thank Dr. Hideaki Ninomiya, Department of Pathology, Kanazawa Medical University, for his assistance with the pathological studies, and Ms. Rieko Nozaki and Ms. Miyuki Yoshita, secretaries of the Department of General Medicine, Kanazawa Medical University, for their assistance with ordering reagents and animals.

References

1. Brown JD, Plutzky J. Peroxisome proliferator-activated receptors as transcriptional nodal points and therapeutic targets. Circulation 2007; 115: 518-33. (Review)
2. Takano H, Nagai T, Asakawa M, *et al.* Peroxisome proliferator-activated receptor activators inhibit lipopolysaccharide-induced tumor necrosis factor-alpha expression in neonatal rat cardiac myocytes. Circ Res 2000; 87: 596-602.
3. Tsuchida A, Yamauchi T, Takekawa S, *et al.* Peroxisome proliferator-activated receptor (PPAR) alpha activation increases adiponectin receptors and reduces obesity-related inflammation in adipose tissue: comparison of activation of PPARalpha, PPARgamma, and their combination. Diabetes 2005; 54: 3358-70.
4. Ichihara S, Obata K, Yamada Y, *et al.* Attenuation of cardiac dysfunction by a PPAR-alpha agonist is associated with down-regulation of redox-regulated transcription factors. J Mol Cell Cardiol 2006; 41: 318-29.
5. Keech A, Simes RJ, Barter P, *et al.* Effects of long-term fenofibrate therapy on cardiovascular events in 9795 people with type 2 diabetes mellitus (the FIELD study): randomised controlled trial. Lancet 2005; 366: 1849-61.
6. Boudina S, Sena S, Theobald H, *et al.* Mitochondrial energetics in the heart in obesity-related diabetes: direct evidence for increased uncoupled respiration and activation of uncoupling proteins. Diabetes 2007; 56: 2457-66.
7. Pedraza N, Rosell M, Villarroya J, *et al.* Developmental and tissue-specific involvement of peroxisome proliferator-activated receptor-alpha in the control of mouse uncoupling protein-3 gene expression. Endocrinology 2006; 147: 4695-704.
8. Boehm EA, Jones BE, Radda GK, Veech RL, Clarke K. Increased uncoupling proteins and decreased efficiency in palmitate-perfused hyperthyroid rat heart. Am J Physiol Heart Circ Physiol 2001; 280: H977-83.
9. Murray AJ, Panagia M, Hauton D, Gibbons GF, Clarke K. Plasma free fatty acids and peroxisome proliferator-activated receptor alpha in the control of myocardial uncoupling protein levels. Diabetes 2005; 54: 3496-502.
10. Bahrami H, Bluemke DA, Kronmal R, *et al.* Novel metabolic risk factors for incident heart failure and their relationship with obesity: the MESA (Multi-Ethnic Study of Atherosclerosis) study. J Am Coll Cardiol 2008; 51: 1775-83.
11. Matsumori A, Sasayama S. Immunomodulating agents for the management of heart failure with myocarditis and cardiomyopathy--lessons from animal experiments. Eur Heart J 1995; 16: 140-3. (Review)
12. Yu F, Chen R, Takahashi T, *et al.* Candesartan improves myocardial damage in obese mice with viral myocarditis and induces cardiac adiponectin. Int J Cardiol 2008; 129: 414-21.
13. Takahashi T, Yu F, Saegusa S, *et al.* Impaired expression of cardiac adiponectin in leptin-deficient mice with viral myocarditis. Int Heart J 2006; 47: 107-23.
14. Kanda T, McManus JE, Nagai R, *et al.* Modification of viral myocarditis in mice by interleukin-6. Circ Res 1996; 78: 848-56.
15. Matsumori A, Kawai C. An experimental model for congestive heart failure after encephalomyocarditis virus myocarditis in mice. Circulation 1982; 65: 1230-5.
16. Kanazawa K, Kawashima S, Mikami S, *et al.* Endothelial constitutive nitric oxide synthase protein and mRNA increased in rabbit atherosclerotic aorta despite impaired endothelium-dependent vascular relaxation. Am J Pathol 1996; 148: 1949-56.
17. Mann DL. Inflammatory mediators and the failing heart: past, present, and the foreseeable future. Circ Res 2002; 91: 988-98. (Review)
18. Niu J, Azfer A, Deucher MF, Goldschmidt-Clermont PJ, Kolattukudy PE. Targeted cardiac expression of soluble Fas prevents the development of heart failure in mice with cardiac-specific

expression of MCP-1. J Mol Cell Cardiol 2006; 40: 810-20.
19. Mann DL. Tumor necrosis factor and viral myocarditis: the fine line between innate and inappropriate immune responses in the heart. Circulation 2001; 103: 626-9.
20. Lopaschuk GD, Folmes CD, Stanley WC. Cardiac energy metabolism in obesity. Circ Res 2007; 101: 335-47. (Review)
21. Shibata R, Ouchi N, Ito M, *et al.* Adiponectin-mediated modulation of hypertrophic signals in the heart. Nat Med 2004; 10: 1384-9.
22. Takahashi T, Saegusa S, Sumino H, *et al.* Adiponectin, T-cadherin and tumor necrosis factor-alpha in damaged cardiomyocytes from autopsy specimens. J Int Med Res 2005; 33: 236-44.
23. Pedraza N, Rosell M, Villarroya J, *et al.* Developmental and tissue-specific involvement of peroxisome proliferator-activated receptor-alpha in the control of mouse uncoupling protein-3 gene expression. Endocrinology 2006; 147: 4695-704.
24. Neubauer S, Horn M, Cramer M, *et al.* Myocardial phosphocreatine-to-ATP ratio is a predictor of mortality in patients with dilated cardiomyopathy. Circulation 1997; 96: 2190-6.
25. Baranowski M, Blachnio-Zabielska A, Gorski J. Peroxisome proliferator-activated receptor alpha activation induces unfavourable changes in fatty acid composition of myocardial phospholipids. J Physiol Pharmacol 2009; 60: 13-20.
26. Finck BN, Han X, Courtois M, *et al.* A critical role for PPA-Ralpha-mediated lipotoxicity in the pathogenesis of diabetic cardiomyopathy: modulation by dietary fat content. Proc Natl Acad Sci U S A 2003; 100: 1226-31.
27. Panzram G. Mortality and survival in type 2 (non-insulin-dependent) diabetes mellitus. Diabetologia 1987; 30: 123-31. (Review)
28. Kenchaiah S, Evans JC, Levy D, *et al.* Obesity and the risk of heart failure. N Engl J Med 2002; 347: 305-13.
29. Buroker NE, Barboza J, Huang JY. The IkappaBalpha gene is a peroxisome proliferator-activated receptor cardiac target gene. FEBS J 2009; 276: 3247-55.
30. Caglayan E, Stauber B, Collins AR, *et al.* Differential roles of cardiomyocyte and macrophage peroxisome proliferator-activated receptor gamma in cardiac fibrosis. Diabetes 2008; 57: 2470-9.

CLINICAL RISK FACTORS IN REGIONAL BRAIN ISCHEMIA USING SINGLE PHOTON EMISSION COMPUTED TOMOGRAPHY

To the Editor: Single photon emission computed tomography (SPECT) brain perfusion imaging has been widely used to diagnose older patients with Alzheimer's disease and other dementia[1,2] and to study cerebrovascular diseases and focal epilepsy and even to determine brain death.[3] Because SPECT provides a qualitative estimate of regional cerebral blood flow (rCBF) according to the radiotracer accumulating in different areas of the brain, the neurological disorders that are tightly coupled with brain metabolism can be detected. Therefore, it is postulated that the rate of delivery of nutrients, which not only the brain disease itself determines, but which other factors such as local circulation and blood components also influence, affects hypoperfusion.

Ninety-five older patients (53 men, 42 women) with suspected stroke were randomly enrolled to undergo the SPECT study. There were no significant differences in age and sex distribution. The SPECT procedure and data analysis, which an experienced technician and two specialists in SPECT blindly performed, were detailed elsewhere.[4] The results of SPECT were shown as two parts: average blood perfusion in two hemispheres (mL/min per 100 g of brain tissue) and regional cerebral perfusion in each brain lobe. For the former, average blood perfusion was defined as positively low perfusion when less than 40 mL/min per 100 g of brain tissue. In addition, all of the diagnostic information was collected from the case history, and information on the blood variables obtained within 3 days of the SPECT detection included red blood cell count (RBC), hemoglobin (Hb), aspartate transaminase, alanine aminotransferase, lactate dehydrogenase (LDH), total protein, albumin, blood urea nitrogen, creatinine, fasting blood glucose (FBG), glycosylated Hb (HbA1c), total cholesterol, high-density lipoprotein cholesterol, low-density lipoprotein cholesterol, and triglycerides. Data were expressed as means ± standard errors. Statistical analysis was performed using the chi-square test, the Student *t*-test, analysis of variance, and the Bonferroni test.

Cerebral ischemia was found in 67 patients, of whom 91.0% had bilateral hemisphere ischemia, especially the men (male, 58.2%; female, 32.8%; $P = .03$) and patients aged 75 and older (≥ 75, 61.2%; <75, 29.8%, $P < .001$). Local ischemia was always detected when patients were diagnosed with cerebral infarction, hypertension, type 2 diabetes mellitus, cervical syndrome, Alzheimer's disease, coronary heart disease, insomnia, carotid artery stenosis, heart failure, reflux esophagitis, arrhythmia, anemia, cerebral hemorrhage, brain atrophy, or depression. Hypoperfusion in the left lobes was significantly more frequent than in the right lobes in patients diagnosed with cerebral infarction (left, 33.6%; right, 26.6%; $P = .03$), hypertension (left, 29.1%; right, 18.4%; $P < .001$), and Alzheimer's disease (left, 18.4%; right, 12.2%; $P = .01$). Moreover, differences were also found in the relationship between blood variables and local hypoperfusion. As shown in Table 1, older patients were at greater risk for local hypoperfusion with lower RBC, Hb, and serum albumin and higher FBG, HbA1c, and LDH.

Lines of evidence have shown that SPECT brain perfusion imaging should be considered to be a preferred test for the diagnosis of some brain diseases since it was introduced as an instrument for the evaluation of rCBF in the early 1980s,[1,3] but a frequent shortcoming of these reports is that the most-typical cases were chosen, and normal older subjects were chosen as controls. Although this improved confidence in the clinical standard of validation, it limited the utility of the results. For example, most older adults with Alzheimer's disease have one or more concomitant diseases, such as cerebrovascular disease, cardiovascular disease, and metabolic disease.

Although the sex and age differences in cerebral blood perfusion are still largely unexplored, it should be considered

Table 1. Blood Variables Collected from Patients with No, Left, and Right Lobe Ischemia According to Single Photon Emission Computed Tomography

Blood Variable	Mean ± Standard Error			*F* Value	*P*-Value
	No Ischemia	Left Ischemia	Right Ischemia		
Red blood cell count (× 10^9/mL)	4.3 ± 0.1	3.7 ± 0.1	3.9 ± 0.1	3.43	.03
Hemoglobin, g/dL	13.9 ± 0.2	12.2 ± 0.1	12.4 ± 0.2	4.24	.01
Aspartate transaminase, U/L	21.4 ± 1.2	25.6 ± 1.1	25.5 ± 1.2	0.56	.57
Alanine aminotransferase, U/L	17.5 ± 1.6	24.4 ± 2.1	24.2 ± 2.1	0.43	.65
Lactate dehydrogenase, U/L	158.9 ± 4.2	207.2 ± 5.0	217.2 ± 6.2	4.31	.01
Total protein, g/dL	6.7 ± 0.1	6.6 ± 0.1	6.7 ± 0.1	0.07	.93
Albumin, g/dL	4.3 ± 0.0	3.7 ± 0.1	3.7 ± 0.1	3.18	.04
Blood urea nitrogen, mg/dL	17.4 ± 1.2	15.1 ± 0.5	16.2 ± 0.7	1.08	.34
Creatinine, mg/dL	0.91 ± 0.05	0.75 ± 0.02	0.71 ± 0.04	1.88	.16
Fasting blood glucose, mg/dL	113.8 ± 5.7	165.1 ± 5.2	157.8 ± 4.8	3.37	.04
Glycosylated hemoglobin, %	4.8 ± 0.2	6.2 ± 0.1	6.1 ± 0.2	3.69	.03
Total cholesterol, mg/dL	204.6 ± 10.4	194.3 ± 3.6	186.0 ± 4.1	1.71	.18
High-density lipoprotein cholesterol, mg/dL	53.7 ± 2.2	53.2 ± 2.8	52.0 ± 3.4	0.04	.96
Low-density lipoprotein cholesterol, mg/dL	105.0 ± 7.6	99.2 ± 4.1	103.8 ± 4.1	0.35	.71
Triglycerides, mg/dL	116.6 ± 11.2	112.1 ± 5.4	103.8 ± 7.3	0.53	.59

in the intervention for patients by combining with other factors. For Japanese people, it has been reported that rCBF is higher in women than in men aged 60 and older and declined significantly with age.[5] The possible foundation might be associated with physical activity such as housework performed by older women but not older men in Japan. More physical activity is associated with greater cerebral blood volume and a lower risk for developing some dementia diseases;[6] hence it is plausible that older women had higher blood perfusion than men younger than 75 in this study. In addition, vascular risk factors, such as hypertension,[7] diabetes mellitus,[8] and even coronary heart disease[9] also negatively affect rCBF. Moreover, SPECT scans were always performed after intravenous injection of the RBC tracer (e.g., 99mTc-labeled RBC) and plasma tracer (e.g., 99mTc-labeled human serum albumin). Hence, the levels of RBC, Hb, and serum albumin could also affect the results of SPECT.

This study found that age, sex, some blood variables, and concomitant diseases significantly influenced the average value of hemisphere blood perfusion and rCBF, which was in part in accordance with previous studies.[5–9] Therefore, it is important that these factors be taken carefully into account for patient enrollment in SPECT studies. Physicians should be aware of risk factors in regional brain ischemia for older patients.

*Rui Chen, MD, PhD**
Union Hospital
Huazhong University of Science and Technology
Wuhan, China

Kanazawa Medical University
Ishikawa, Japan
Himi Municipal Hospital
Toyama, Japan

*Fengxia Liang, MD, PhD**
Hubei University of Traditional Chinese Medicine
Wuhan, China

Kei-Ichiro Ishigami, MD, PhD
Tsugiyasu Kanda, MD, PhD
Kanazawa Medical University
Ishikawa, Japan

Himi Municipal Hospital
Toyama, Japan

Li Zeng, MD
Kanazawa Medical University
Ishikawa, Japan

Atsushi Saito, MD
Masayuki Hasegawa, MD
Naohiro Yamashita, MD
Tomohiko Itoh, MD
Toshikazu Kigoshi, MD
Yoichi Izumi, MD
Noboru Takekoshi, MD
Kanazawa Medical University
Ishikawa, Japan
Himi Municipal Hospital
Toyama, Japan

Shigeto Morimoto, MD, PhD
Kanazawa Medical University
Ishikawa, Japan

*These authors contributed equally to this work.

ACKNOWLEDGMENTS

Conflict of Interest: The editor in chief has reviewed the conflict of interest checklist provided by the authors and has determined that the authors have no financial or any other kind of personal conflicts with this paper.

Author Contributions: All authors contributed to this letter.

Sponsor's Role: None.

REFERENCES

1. Bergman H, Chertkow H, Wolfson C et al. HM-PAO (CERETEC) SPECT brain scanning in the diagnosis of Alzheimer's disease. J Am Geriatr Soc 1997;45:15–20.
2. Read SL, Miller BL, Mena I et al. SPECT in dementia: Clinical and pathological correlation. J Am Geriatr Soc 1995;43:1243–1247.
3. Therapeutics and Technology Assessment Subcommittee of the American Academy of Neurology. Assessment of brain SPECT. Neurology 1996;46:278–285.
4. Hanyu H, Sakurai H, Hirao K et al. Unawareness of memory deficits depending on cerebral perfusion pattern in mild cognitive impairment. J Am Geriatr Soc 2007;55:470–471.
5. Takeda S, Matsuzawa T, Matsui H. Age-related changes in regional cerebral blood flow and brain volume in healthy subjects. J Am Geriatr Soc 1988;36:293–297.
6. Scarmeas N, Luchsinger JA, Schupf N et al. Physical activity, diet, and risk of Alzheimer disease. JAMA 2009;302:627–637.
7. Efimova IY, Efimova NY, Triss SV et al. Brain perfusion and cognitive function changes in hypertensive patients. Hypertens Res 2008;31:673–678.
8. Schmidt R, Launer LJ, Nilsson LG et al. Magnetic resonance imaging of the brain in diabetes: The Cardiovascular Determinants of Dementia (CASCADE) Study. Diabetes 2004;53:687–692.
9. Ouchi Y, Yoshikawa E, Kanno T et al. Orthostatic posture affects brain hemodynamics and metabolism in cerebrovascular disease patients with and without coronary artery disease: A positron emission tomography study. Neuroimage 2005;24:70–81.

CENTENARIAN STROKE TREATED WITH REHABILITATION THERAPY

To the Editor: A 104-year-old, right-hand-dominant man who awoke with aphasia and right-sided weakness was admitted to the emergency department in February 2006. He had a previous history of hypertension, lacunar cerebellum stroke, implanted cardiac pacemaker, and urothelial carcinoma stage G2 pT1 (treated by transurethral resection in 2005). Before admission, he had been independent in activities of daily living (ADLs) (Barthel Index: 100/100) and able to ambulate independently with a walking stick. He enjoyed an active lifestyle, including walking every day. He had no cognitive alterations.

On hospital admission, he had severe motor deficit with right hemiplegia, mixed aphasia, and delirium. Computerized tomography showed an acute infarct in the left anterior middle cerebral artery. Physical therapy was not initially indicated because of delirium, severe flaccid right-sided weakness, and lack of sitting balance.

He was admitted to a subacute care unit for follow-up. He required major assistance (2 people) to stand, lacked sitting balance, and was completely dependant for personal

J Physiol Sci (2010) 60:383–388
DOI 10.1007/s12576-010-0099-6

ORIGINAL PAPER

Evaluations of dementia by EEG frequency analysis and psychological examination

Hiroshi Yoshimura · Shigeto Morimoto · Masashi Okuro · Natsuki Segami · Nobuo Kato

Received: 20 August 2009 / Accepted: 26 May 2010 / Published online: 18 June 2010

Abstract In order to evaluate the stage of dementia, we focused attention on EEG rhythms and Hasegawa-dementia-rating scale (HDS-R). Frontal EEGs were recorded from dementia patients and normal controls during music and photo-image stimulations, and frequency analysis was performed. In the controls, profiles of rhythm pattern during music stimulation seemed to be markedly different from those during photo-image stimulation. In contrast, in dementia patients, it was difficult to find those differences. Interestingly, as HDS-R decreases, the variability of rhythm patterns also decreases. These results suggest that a decrease in cognitive function might be related to a decrease in the ability to generate various cortical rhythm patterns.

Keywords EEG · Frequency analysis · Dementia · HDS-R · Music · Photo image · Theta frequency band · Alpha frequency band

Introduction

Dementia is considered to be a disease of cognitive dysfunction, but not to be an exaggerated condition of normal aging [9, 10]. Dementia has several stages of cognitive dysfunction, and has the feature of gradual exacerbation. Mild cognitive impairment (MCI) tends to convert into dementia, and once suffering from the dementia, it is difficult to improve cognitive function [11, 14]. Therefore, it is important to diagnose the early stage of cognitive dysfunction for prevention and treatment of dementia.

In order to evaluate dementia, Hasegawa-dementia-rating scale (HDS-R) and mini-mental state examination (MMSE) have been developed, and are generally used, as in psychometric assessment. Recently, for morphological and metabolic assessments, diagnostic criteria have been under development by using brain-imaging techniques, such as functional MRI and FDG-PET [7, 10]. These methods enable us to investigate from the surface to deep areas of the brain, and to provide information about regional atrophy and homodynamic changes. However, these medical examinations may to some extent impose stress on the patients. Among electrophysiological methods, evaluations of cognitive dysfunction by using event-related potential (ERPs) or electroencephalographic (EEG) frequency analysis have been developed [1, 6]. Although electrophysiological activities reflect neuron activities in the brain, it is presently difficult to evaluate precise stages of dementia.

For screening cognitive dysfunction, less invasive and less stressful examinations that reflect brain function are preferred. In this respect, we have focused attention on EEG frequency analysis, and psychological assessment, HDS-R, in the present study.

Methods

Sixteen outpatients, whose ages were 73.7 ± 4.8 years (mean ± SD), from Kanazawa Medical University

H. Yoshimura (✉) · N. Segami
Department of Oral and Maxillofacial Surgery, Kanazawa Medical University, Uchinada-cho, Ishikawa 920-0293, Japan
e-mail: hyoshimu@kanazawa-med.ac.jp

H. Yoshimura · N. Kato
Department of Physiology, Kanazawa Medical University, Uchinada-cho, Ishikawa 920-0293, Japan

S. Morimoto · M. Okuro
Department of Geriatrics, Kanazawa Medical University, Uchinada-cho, Ishikawa 920-0293, Japan

Hospital, diagnosed as having dementia were included in this study. All patients underwent the psychological test of HDS-R. A medical doctor of geriatrics performed the psychological test. Ten healthy controls whose ages were 58.0 ± 13.8 years (mean ± SD) were recruited, and also underwent the neuropsychological test of HDS-R. All experiments were undertaken with the understanding of the subjects.

EEGs were recorded from frontal region of the scalp, by using EEG recorder, FM-515A (Futek, Tokyo, Japan). Frequency analyses of EEGs were performed with PRLUXII (Futek). Frequency bands were divided into theta (4–7 Hz), alpha1 (7–9 Hz), alpha2 (9–11 Hz), alpha3 (11–13 Hz) and beta (13–30 Hz). Data were collected for every 1 s. Occupancy rate of each frequency band was calculated as follows. Power of each frequency band was divided by the sum of the powers of all frequency bands, and the ratio was defined as a unit occupancy rate (%). Activities of each frequency band were firstly assessed by the unit occupancy rate per second. Then the unit occupancy rates through one course of session (180 s) were averaged, and we adopted the data of "occupancy rate" (%). Hereafter in this study, we refer to the averaged rate as occupancy rate.

Participants sit in the body sonic chair (Refresh 1 Excellent, Tokyo, Japan), and listen to the music in comfort. In front of the chair, a 150 cm × 100 cm screen was located at 2 m distance on which patients were able to see images of photographs. Images were projected on the screen through a PC Projector, EMP-1705 (Epson, Tokyo, Japan) connected to a PC. Famous Japanese standard songs in the category of country music, "Furusato" and "Nanatsuno-ko", were selected from Japanese music CDs, and presented as an auditory stimulation. Photographs of scenic Japanese spots were presented as visual stimulation. The auditory and visual stimulation were applied for 180 s each.

During one session (180 s), EEG epochs with artifacts were identified (threshold: 5 μV), and artifact-free EEG epochs were adopted for analysis. Thus, the "unit occupancy rate" through one session was not 180 but 154.3 ± 21.5 (mean ± SD, $n = 16$) in the case of the auditory stimulation for dementia patients, 133.8 ± 31.7 (mean ± SD, $n = 16$) in the case of visual stimulation for dementia patients, 163.8 ± 14.6 (mean ± SD, $n = 10$) in case of auditory stimulation for healthy controls, and 156.9 ± 26.8 (mean ± SD, $n = 10$) in case of visual stimulation for healthy controls.

Local institutional ethics committees of Kanazawa Medical University approved the present study, and all experiments were performed in accordance with the ethical standards laid down in the 1964 Declaration of Helsinki and the Guiding Principles for the Care and Use of Animals in the Field of Physiological Sciences. All persons gave their informed consent prior to their inclusion in the study.

Results

EEGs were recorded from a healthy control during both music and photo-image stimulations, and frequency analysis was performed. The occupancy rate of each frequency band is shown in Fig. 1a. In the case of the music stimulation, the occupancy rate of the alpha2 band was dominant compared with those of other frequency bands, whereas in the case of the photo-image stimulation, the occupancy rates of the theta and beta bands were relatively dominant compared with those of other frequency bands. The profiles of the rhythm pattern during music stimulation and during photo-image stimulation seemed to be markedly different.

In the same way, EEGs were recorded from a dementia patient during both music and photo-image stimulation, and frequency analysis was performed. The occupancy rate of each frequency band is shown in Fig. 1b. On comparing the occupancy rates of the five frequency bands obtained from a dementia patient with those obtained from a healthy control, it is difficult to find marked differences of rhythm pattern in the dementia patient (Fig. 1b). These results show that different patterns of frontal EEG rhythm seem to be generated in a normal control when different sensory stimulations are applied, whereas, in a dementia patient, it might be difficult to generate diverse patterns of frontal EEG rhythm.

Occupancy rates of theta frequency bands obtained from 10 normal controls are plotted together in Fig. 2a (Theta), and those obtained from 16 dementia patients are plotted together in Fig. 2b (Theta). In the same way, occupancy rates of other frequency bands are plotted in Fig. 2a, b. By comparing the occupancy rates obtained from normal with those obtained from dementia patents, occupancy rates elicited by music stimulation in normal controls tended to be different from those elicited by photo-image stimulation in a few frequency bands, whereas, in dementia patients, it is difficult to find differences of occupancy rates between the music and photo-image stimulations. These findings are statistically evaluated as follows.

In order to quantify the variability of rhythm patterns, the variation score of each frequency band was obtained by subtracting the occupancy rate in the case of photo-image stimulations from the occupancy rate in the case of music stimulations, which was executed for the five frequency bands. The data obtained from individual subjects were averaged, and are plotted in Fig. 3. In this figure, the variation score near zero indicates that there is a small difference between the occupancy rate during music stimulation and that during photo-image stimulation. Analysis of variance (ANOVA) was used to evaluate the statistical significance of the variation scores in all five frequency-bands. In the dementia group, there is no statistical difference ($F = 2.67, P = 0.038$), whereas in the normal group, there

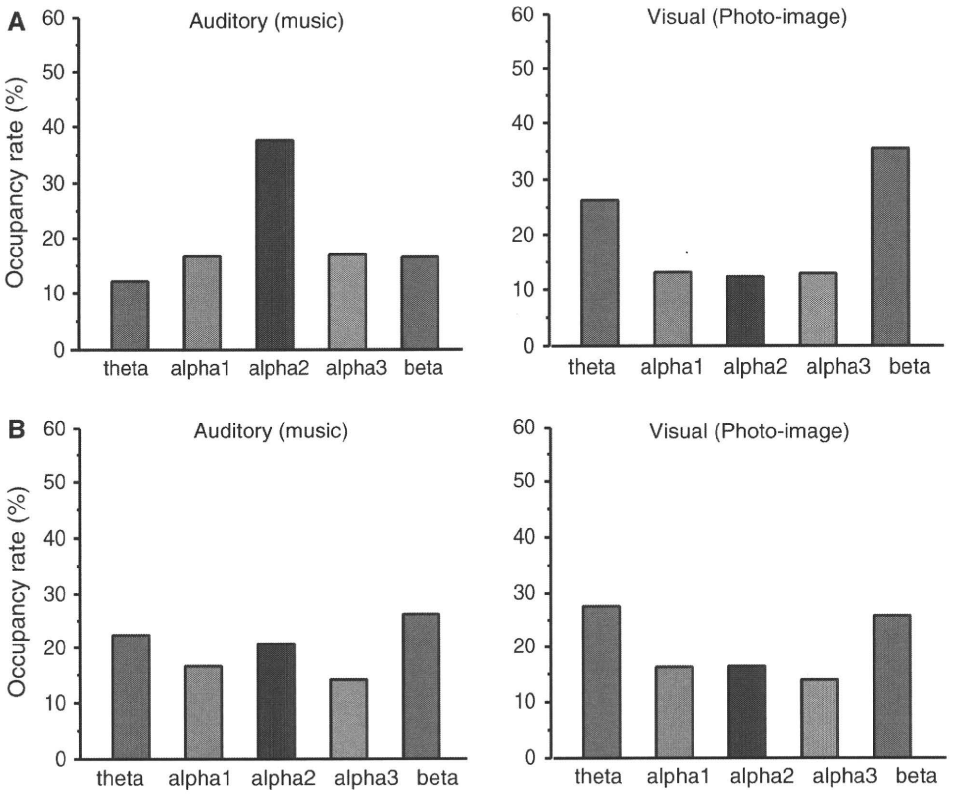

Fig. 1 Occupancy rates of the five frequency bands during music stimulation compared with those during photo-image stimulation. The frequency bands of interests are theta, alpha 1, 2, 3 and beta. Data were obtained from **a** a normal control and **b** a dementia patient

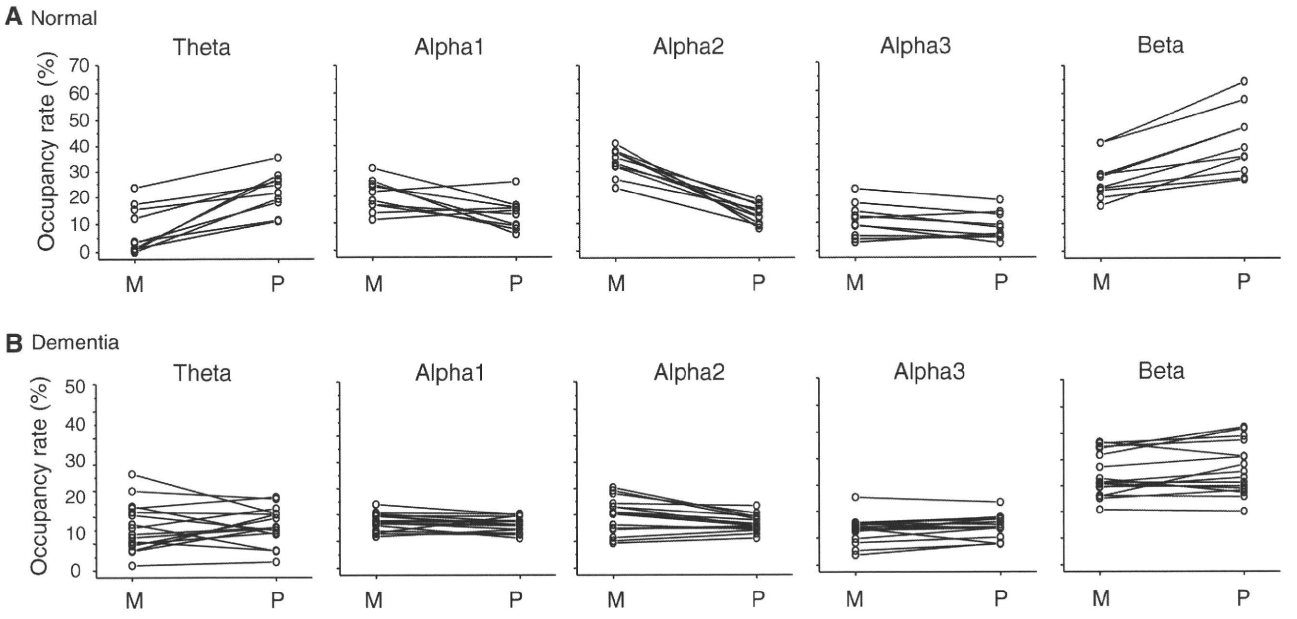

Fig. 2 Comparing the differences between occupancy rates of the five frequency bands during music and those during photo-image stimulation. Data were obtained from **a** 10 normal controls and **b** 16 dementia patients. Individual sets of occupancy rate between music and photo-image stimulations are plotted for 5 frequency bands of interest. *M* Music stimulation, *P* photo-image stimulation

is a large statistical difference ($F = 53.6$, $P = 1.1 \times 10^{-16}$), when the level of significance is 0.01. The data show that variability of rhythm patterns was much larger in normal controls than in dementia patients.

In the next analysis, correlations between the variability of rhythm patterns and HDS-R were investigated. In order to evaluate the variability of rhythm patterns, the variation score was used as described above. Variation scores in the

theta frequency band were plotted against HDS-R in Fig. 4 (Theta). In the same way, variation scores about other frequency bands were plotted against HDS-R in Fig. 4 (Alpha1, Alpha2, Alpha3, and Beta). These analyses indicate that there is a negative correlation between variation score and HDS-R in the theta frequency band ($R = -0.77$, $P < 0.0001$) and in the beta frequency band ($R = -0.56$, $P = 0.0027$), and a positive correlation in the alpha2 frequency band ($R = 0.88$, $P < 0.0001$), when the level of significance is 0.01. Thus, in the theta and beta frequency bands, as HDR-S decreases, the variation score also decreases, and in the alpha2 frequency band, as HDR-S decreases, the variation score increases. These results also show that, as HDR-S decreases, the variation scores of the theta, alpha2 and beta frequency bands deviates from zero. This finding suggests that, as cognitive function decreases, the variability of rhythm patterns also decreases.

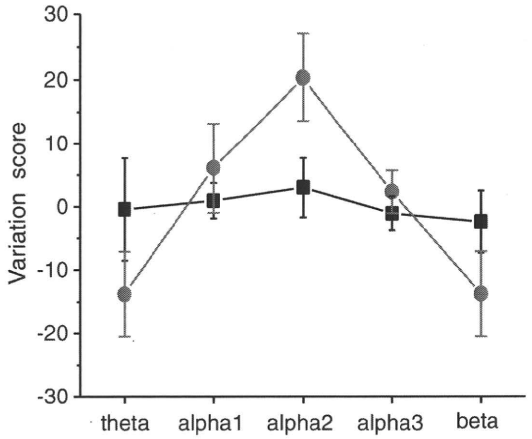

Fig. 3 Evaluation of EEG rhythm variations by calculating the variation score, where the occupancy rates during photo-image stimulations were subtracted from occupancy rates during music stimulations. The variation scores obtained from normal controls ($n = 10$) and dementia patients ($n = 16$) were averaged and are plotted (mean ± SD). *Circles* indicate data from normal controls, and *squares* indicate data from dementia patients. Note that variation scores distant from zero indicate that there is a large difference between the two occupancy rates

In the next analysis, correlations between the variability of rhythm patterns and age were investigated by using data from both healthy controls and the dementia group. The same data of variation scores plotted in Fig. 4 were used. Variation scores in the theta frequency band were plotted against age in Fig. 5 (Theta). In the same way, variation scores about other frequency bands were plotted against HDS-R in Fig. 5 (Alpha1, Alpha2, Alpha3, and Beta). These analyses indicate that there is a negative correlation between variation score and age in the alpha3 frequency band ($R = -0.56$, $P = 0.003$), but not in the other frequency bands, when the level of significance is 0.01.

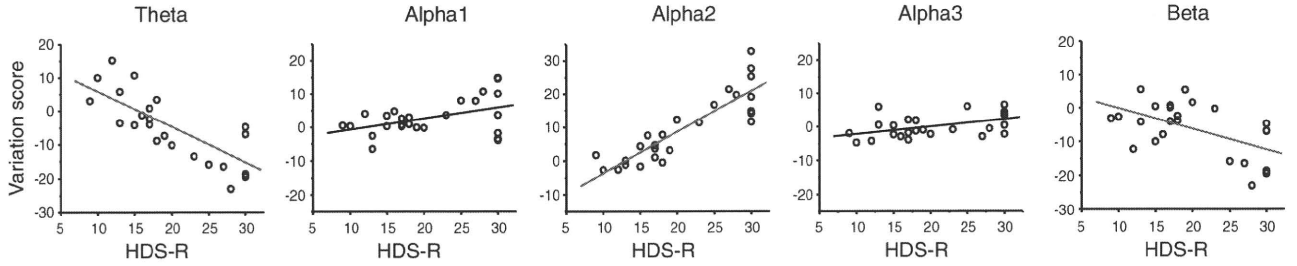

Fig. 4 Relationships between the variation score and HDS-R. The variation scores of the five frequency bands of interests obtained from normal controls ($n = 10$) and dementia patients ($n = 16$) are plotted against HDS-Rs, and linear fittings performed. Note that there are correlations between variation scores and HDS-R in the theta ($R = -0.77$, $P < 0.0001$), alpha2 ($R = 0.88$, $P < 0.0001$) and beta frequency bands ($R = -0.56$, $P = 0.0027$), when the level of significance is 0.01

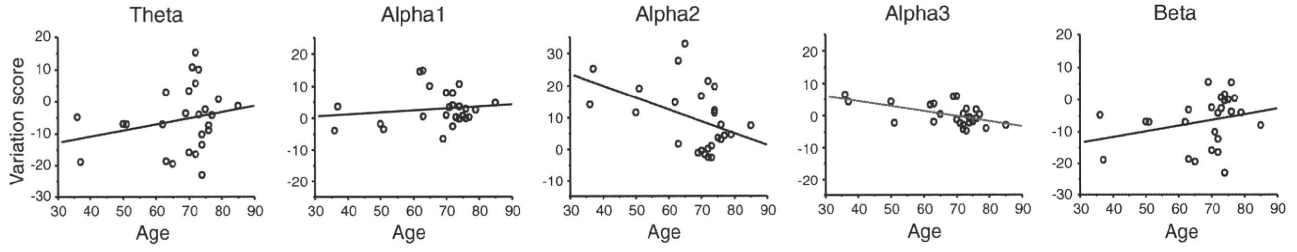

Fig. 5 Relationships between the variation score and age. The variation scores of the five frequency bands of interests obtained from normal controls ($N = 10$) and dementia patients ($N = 16$) were plotted against age, and linear fittings were performed. Note that there are correlations between variation score and age in alpha3 frequency bands ($R = -0.56$; $P = 0.003$), when level of significance is 0.01